Lab on a Chip

ARTICLE

Development of a Point-of-Care Diagnostic for Influenza Detection with Antiviral Treatment Effectiveness Indication

Received 00th January 20xx,
Accepted 00th January 20xx

DOI: 10.1039/x0xx00000x

www.rsc.org/

Richard C. Murdock[a,b], Karen M. Gallegos[c,d], Joshua A. Hagen[a], Nancy Kelley-Loughnane[a], Alison A. Weiss[c], and Ian Papautsky[b]

Currently, diagnosis of influenza is performed either through tedious polymerase chain reaction (PCR) or through rapid antigen detection assays. The rapid antigen detection assays available today are highly specific but not very sensitive, and most importantly, lack the ability to show if the strain of influenza detected is susceptible to antiviral agents, such as Tamiflu and Relenza. The ability to rapidly determine if a patient has an infectious disease and what type of treatment the infection will respond to, would significantly reduce the treatment decision time, shorten the impact of symptoms, and minimize transfer to others. In this study, a novel, point-of-care style µPAD (microfluidic paper-based diagnostic) for influenza has been developed with the ability to determine antiviral susceptibility of the strain for treatment decision. The assay exploits the enzymatic activity of surface proteins present on all influenza strains, and potential false positive responses can be mitigated. A sample can be added to the device, distributed to 4 different reagent zones, and development of the enzymatic substrate under different buffer conditions takes place on bottom of the device. Analysis can be performed by eye or through a colorimetric image analysis smartphone application.

Introduction

Influenza accounts for nearly 200,000 hospitalizations and 36,000 deaths each year in the United States alone, with approximately 500,000 deaths worldwide [1]. Considering the rapid course of viral action and severity of symptoms, early detection of influenza is critical, especially in certain subpopulations. The elderly, young children, immunosuppressed patients, individuals with preexisting medical conditions, and pregnant women are particularly susceptible to severe cases of infection. Additionally, in cases where individuals are in close daily contact with a small group of people, influenza can spread rapidly and cause substantial illness and loss of workdays. CDC reports that 111 million workdays at a $7 billion cost are lost annually in the U.S. due to influenza sick days and lost productivity [2]. In a military setting, such as a small base, this could significantly impact the preparedness of military units [3].

Influenza contains two antigenic surface glycoproteins, hemagglutinin (HA) and neuraminidase (NA), which are responsible for binding to a host cell and facilitating virus uptake and release of newly synthesized viruses. NA activity is essential for efficient replication of influenza; it increases access to the cell surface by removing decoy receptors on mucins, cilia and the cellular glycocalyx [4, 5]. NA facilitates the release of newly synthesized viruses from host cells, preventing self-aggregation of virus and guaranteeing virus spread [6, 7]. HA and NA constantly undergo mutations to their genetic sequences. During antigenic drift, influenza accumulates mutations in all gene segments. During antigenic shift, influenza exchanges HA or NA genome segments from different influenza viruses (e.g. pigs and birds) resulting in new virus subtypes. Antigenic drift and shift rapidly changes the influenza virus, making characterization and detection of influenza strains challenging. Oseltamivir (Tamiflu®) and zanamivir (Relenza®) are currently the only anti-influenza drugs approved for treatment in humans. NA-inhibitors (NAIs) halt influenza infection by limiting replication to only one infectious cycle [8]. NAI resistance has emerged in influenza virus, with resistance to oseltamivir more commonly seen than resistance to zanamivir.

Currently, influenza is primarily diagnosed either through polymerase chain reaction (PCR) or through rapid antigen detection tests (RDTs). PCR is a complicated laboratory procedure that must be performed by well-trained personnel, takes 2-4 h to complete, and requires expensive laboratory equipment. Additionally, PCR requires the proper viral primers for the assay to work, which constantly need to be re-validated due to the constant change of the viral genome. The RDTs currently available are based on lateral flow assay (LFA) platforms, meaning they are a point-of-care (POC) device, and are able to provide a result in 15-20 min. However, these RDTs lack the ability to show if the strain of influenza detected is susceptible to antiviral agents, and offer different levels of differentiation of types of influenza (A only, A or B, A and B). In

[a]711 HPW/RHXBC, Human Signatures Branch, Airman Systems Directorate, 711th Human Performance Wing, Wright-Patterson AFB, OH, USA.
[b]BioMicroSystems Lab, Department of Electrical Engineering and Computing Systems, University of Cincinnati, Cincinnati, OH, USA.
[c]Department of Molecular Genetics, Biochemistry, and Microbiology, University of Cincinnati, Cincinnati, OH, USA.
[d]Department of Microbiology and Immunology, Midwestern University, Downers Grove, IL, USA

Electronic Supplementary Information (ESI) available: [details of any supplementary information available should be included here]. See DOI: 10.1039/x0xx00000x

reality, antibody-based RTDs often show deficient sensitivity for detection, particularly when new influenza strains naturally emerge [9] as previously reported for H1N1pdm/09 pandemic and H3N2v [10-13]. Ultimately, while these tests are highly specific (>90%), they can only provide the primary care provider with confirmation of influenza presence, not activity level.

Paper microfluidic analytical devices have emerged in recent years [14, 15], leading to the development of a number of POC analyses, including HIV chips [16, 17], paper-based ELISA [18-21] and low-cost colorimetric diagnostic assays [22-27]. Of specific interest are the microfluidic paper-based analytical devices (μPADs). These are paper devices that contain multiple hydrophobic patterned layer to guide a sample horizontally and vertically through a device while performing various processing steps, such as sample division, adjustment of sample pH, filtering, and even sequential reagent additions. In addition to being inexpensive and relatively easy to manufacture, they can be quite robust with reagent storage for real-world POC use [28]. For sample detection and measurement, colorimetric, fluorometric, chemilumescent, and electrochemical methods have all been successfully implemented with the μPAD format [29, 30].

In this work, as an alternative to antibody-based diagnostic tests, we used a new approach to develop a theranostic device for influenza based on the properties of the viral NA. We confirmed NA activity at various pH levels, in the presence of cations or chelators, to determine a common buffer condition that would detect both influenza A and B on a paper-based platform. We also observed strain dependent pH responses that could be used to quickly "subtype" a suspected influenza sample. Additionally, NAIs were incorporated into the assay to determine strain-dependent NAI resistance. Once the proper assay conditions were determined, along with the reagent storage conditions, we incorporated these into a one-step, multi-layer, microfluidic paper-based analytical device for POC applications.

Materials and methods

Chemicals and Solutions. The 5-Bromo-4-chloro-3-indoyl-α-D-N-acetylneuraminic acid (X-NeuNAc) was obtained from Santa Cruz Biosciences. Purified influenza A H1N1 (A/California/07/09 H1N1 or A(H1N1)pdm09) Neuraminidase protein was obtained from Sino Biological. Pullulan from *Aureobasidium pullulans* was obtained from Sigma Aldrich. Sodium acetate, sodium tetraborate, phosphate buffered saline (PBS), Tris(hydroxymethyl)-aminomethane (Tris), calcium, Ethylenediaminetetraacetic acid (EDTA), Cetyltrimethylammonium bromide (CTAB), and Bovine serum albumin (BSA) were all sourced through Sigma Aldrich.

Virus and Bacterial Stocks. Live virus and bacterial stocks were used from frozen storage from Dr. Weiss' group at the University of Cincinnati Medical Campus. Influenza viruses were initially obtained from the Centers for Disease Control. Viral samples were propagated in MDCK cells and the supernatants were harvested by centrifugation after cytopathogenic effects were observed and stored at -80°C. All viral and bacterial work was completed in a bio-safety level (BSL) 2 facility with proper personal protective equipment (PPE). In this study we used five different influenza strains A/California/07/09 H1N1 A(H1N1)pdm/09, A/Brisbane/59/07-Like H1N1 (H1N1/07-R), A/Brisbane/10/07-Like (H3N2/07-S), A/Texas/12/07 (H3N2/07-R), B/Florida/04/06 (Yama/08-S); and two parainfluenza strains. Human Parainfluenza Virus type 2 (HPIV2) and Human para influenza virus type 1 were obtained through the NIH Biodefense and Emerging Infectious Diseases Research Resources Repository, NIAID, NIH. *Streptococcus pneumoniae* strain ATCC 49619 (Strep) was kindly provided by Vicki Stegner at UC Health University Hospital, Cincinnati, OH. In order to easily differentiate each group, in this study, we indicated oseltamivir-resistant influenza by –R and oseltamivir-sensitive influenza by –S at the end of each abbreviation of influenza strain. Influenza A and B, as well as parainfluenza virus samples were thawed and diluted 1:3 from frozen stocks into sterile DI H_2O. *Streptococcus pneumonia*e was thawed and cultured on a blood agar plate overnight at 37°C until colonies were observed. The colonies were harvested and, after dilution, the final working solution absorption was 0.1 O.D. (600 nm) which is ~$2x10^7$ CFU/mL. This was then diluted 1:1500 into sterile DI H_2O. Supernatants of mock infected MDCK cells were used as a negative control.

Printing of Paper 96-well Plates. Procedure previously described in Murdock *et al.* [20]. Briefly, a 'negative' image of a 96-well plate was printed using a Xerox ColorQube 8570N solid wax ink printer. The wax image of the 96-well plate was printed onto Whatman #1 filter paper, which was then placed onto a hot plate which allowed the wax to fully melt through the wax paper evenly across the entire plate (~4 min). Final well diameters after melting were ~3.8 mm.

Neuraminidase Activity Assays. After creating the 96-well paper plate via the wax printing method, the plate was trimmed to fit inside a large culture dish, with a small square culture plate inside the larger round culture plate to act as a support and suspend the paper plate. Initially, 10 μL of the appropriate buffer solution containing X-NeuNAc substrate was added to each well. This was immediately followed by the addition of 3 μL of the viral or bacterial diluted solution (1:3 for viral samples, 1:1500 for *S. pneumoniae*). Sodium acetate buffer (50 mM, 1X) was used for studies at pH 4, PBS (1X) was used for studies at pH 7, and Tris buffer (50 mM, 1X) was used for studies at pH 9. During μPAD development, a buffer substitution was made, sodium borate (50mM, 1X) for Tris, to increase buffer stability at pH 9 during dry storage, device assembly, and subsequent resuspension. Buffer studies were performed (unpublished data) to confirm that assay performance matched the results previously observed with the Tris buffer. All buffers contained 200 mM NaCl and 14.82 mM X-NeuNAc substrate. The "+" after a buffer name indicates the presence of 0.1 mM Ca^{2+}, whereas the "-" indicates the presence of 5 mM EDTA chelator. For all 96-well plate assays, a small amount of sterile DI H_2O was added to the bottom of the culture dish to prevent the assay from drying out too quickly by creating a humid environment unless otherwise noted. The cover was then placed on the culture dish and the assay was left to incubate in the BSL-2 hood overnight at either ambient temperature (18-20°C) or a heated, non-humidified incubator (37°C). After 10 h of incubation, the samples

were imaged with a digital camera. All assay trials were performed in duplicate with 3 independent replicates (n=6).

Reagent Preservation and Storage. Using the previously described assay procedure for 96-well plate format, Pullulan was added at increasing concentrations (1, 2.5, 5, 7.5, and 10% w/v) to the various pH buffers and X-NeuNAc substrate with purified NA to determine if there was any potential interference with the assay performance. The samples were allowed to react until dried and were then imaged to compare performance.

For determination of the storage buffer concentration, 6.5 µL the substrate and the appropriate buffer condition with increasing concentrations of Pullulan (1, 2.5, 5, 7.5, and 10% w/v) were dried onto the paper 96-well plate and allowed to sit in open air at room temperature for 3 days. Afterwards, 10 µL of DI H2O and 3 µL of purified NA (100 U/mL) were spotted onto the dried substrate areas and allowed to react for ~3 h. The samples were imaged and analyzed to determine relative NA activity levels. Again, all trials were performed in duplicate with 3 independent replicates (n=6).

Influenza Microfluidic Paper-based Analytical Device (µPAD). For the distribution and development layers, printable images which define the wax areas were made from the AutoCAD drawings and printed onto the Whatman #1 filter paper using the wax printing method described previously for the 96-well plate. The wax was subsequently heated to flow the wax through the entire cross-section of the filter paper. After printing, both the distribution and development layers were cut using a laser cutting printer (Universal Laser Systems VLS3.50) for assembly purposes to allow for 9 µPADs to be fabricated at one time. Additionally, the laser cutting printer was used to cut the sample inlet hole out of the top lamination layer (Staples 5 mil Lamination Sheets). Next, the development layer was loaded with 6.5 µL of the X-NeuNAc substrate in the appropriate buffer along with 7.5% w/v Pullulan. Finally, all layers were assembled and passed through a hot roll laminator (Western Magnum Model # XRL-120), followed by device cutting from the master using the laser cutting printer (Figure 1). To evaluate samples, 30 µL of the previously discussed virus and bacterial sample dilutions were pipetted into the top sample port on the µPAD. Three independent trials were performed for each sample (n=3).

Image Analysis. Images were captured using a Panasonic Lumix DMC-ZS5 digital camera and processed using ImageJ (NIH). An average RGB value was obtained for each test spot by selecting the test spot area, excluding the transition from color to gray-black wax at the edges, and then selecting the color histogram function in ImageJ. These average RGB values were then transferred into an Excel workbook which converted each value into the corresponding CIE 1931 color space coordinates (and ΔCIE) as described in our previous paper[20]. For the final device images, it was found that using only the x-axis coordinate of the ΔCIE value gave a very precise indication of the amount of color change. Therefore, any blue color shift due to the reduction of the substrate would be shown as a positive value.

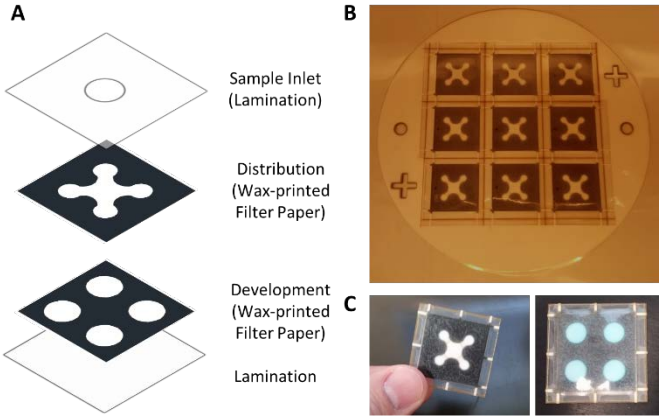

Figure 1. Influenza µPAD Design and Fabrication. (A) Exploded view of the influenza µPAD construction. (B) Image of the influenza µPADs after lamination and prior to individual device cutting. Nine devices can be manufactured at once. (C) Finished influenza µPAD, front and back.

Results and Discussion

Neuraminidase Activity Assay Optimization

Our initial studies show the feasibility of detecting influenza based purely on NA activity on a microtiter plate using fluorogenic sialic acid analog (MUNANA) as the substrate instead of the colorimetric substrate (X-NeuNAc) which we use for the development of the influenza µPAD. Both substrates contain sialic acid, that is recognized by influenza NA. The colorimetric substrate was chosen to make analysis easier, whether by visual interpretation or image analysis methods, since fluorogenic substrates would require more complicated instrumentation for analysis.

Four different strains of influenza A (A(H1N1)pdm/09-S, H1N1/07L-R, H3N2/07L-S, and H3N2/07-R), one influenza B strain (Yamagata), and two potentially assay interfering upper respiratory infectious pathogens (HPIV-2 and *S. pneumoniae*) were examined in this study. These infectious diseases were chosen to represent a cross-section of the potential influenza strains which could be encountered. Additionally, since NA is also produced by other common human respiratory pathogens [31] that may be present in a mucosal sample, specifically parainfluenza virus [32] and bacteria such as *S. pneumoniae* [33-35], we incorporated these as potential false positive tests to determine if the assay could distinguish between influenza and other respiratory pathogens.

To verify operation of the colorimetric NA assay on the paper platform, we began by using just one influenza A subtype (H1N1/07L-R) to determine a baseline response for comparison of detection performance. These experiments were performed on a wax-printed, 96-well plate format device previously described[20]. While the physical layout of this paper-based device exactly matched the dimensions (well spacing) of a conventional 96-well microplate, there was a substantial reduction in the required fluid volume per test. Whereas a conventional microplate normally required >60 µL of fluid per

well, the paper-based plate only required a minimum of 3 µL to fill the test area.

First, it was necessary to determine if the assay could develop in ambient (dry) conditions or if it was necessary to keep the assay in a humidified state to prevent drying prior to complete development. The "humid" condition was made by adding a small amount of DI H_2O to the bottom the culture dish prior to adding the cover. No water was added to the "dry" dish prior to covering. It was observed that while the "dry" assay did produce a visible response; it was very weak compared to the "humid" assay response (Figure S1). From this point on, all experiments were performed under the "humid" conditions to maximize responses.

We examined the buffer strengths for the 3 different pH conditions to verify that we had the optimal buffer conditions for the NA assay. Sodium acetate buffer (50 mM (1X), 100 mM (2x), and 150 mM (3X)) was used for studies at pH 4, PBS (1X, 2X, and 3X) was used for studies at pH 7, and Tris(hydroxymethyl)aminomethane (Tris) buffer (50 mM (1X), 100 mM (2x), and 150 mM (3X)) was used for studies at pH 9. All buffers contained 200 mM NaCl and 14.82 mM (3.33X) X-NeuNAc substrate. The "+" after a buffer name indicates the presence of 0.1 mM Ca^{2+}, whereas the "-" indicates the presence of 5 mM EDTA. From the results it was found that increasing buffer strength did not have a significant effect on assay response; however, a very minor increase was observed at the 2X PBS condition, but was not enough to justify changing buffer conditions (Figure S2). All buffer strengths were kept at their 1X concentration from this point forward.

Incubation temperature and substrate concentration were investigated to determine if any enhancements in assay development could be observed. Room temperature incubation (~20°C) and a non-humidified cell incubator incubation (37°C) were compared over 10 h, as well as increased X-NeuNAc concentrations 14.82 mM (3.33X) and 22.23 mM (5X). It was expected to see enhanced assay response with both increased temperature and substrate concentration, which is confirmed by the results in Figure S3; however, it was not expected to see such an enhanced response at 37°C for the pH 9+ condition. While the elevated temperature will enhance most enzyme-substrate reaction rates due to higher system energy and reaction rates, the enhanced response at pH 9+, 37°C could also be due to buffer pH change since the H1N1 seems to respond similarly to the pH 7+ condition at 37°C.

Lastly, to determine if increased temperature resulted in decreased time to detection, a time course study was performed with the H1N1-S1R at 20°C and 37°C. The elevated temperature did significantly reduce the time to a positive result (i.e. enough blue development to detect significantly above background) by reducing assay time from ~400 minutes (20°C) to ~150 minutes (37°C) (Figure S4). Nevertheless, we proceeded with all experiments at room temperature (~20°C) due to a more predictable assay response and the future POC use of the assay as a user would not want to have to have access to an incubator to develop the device.

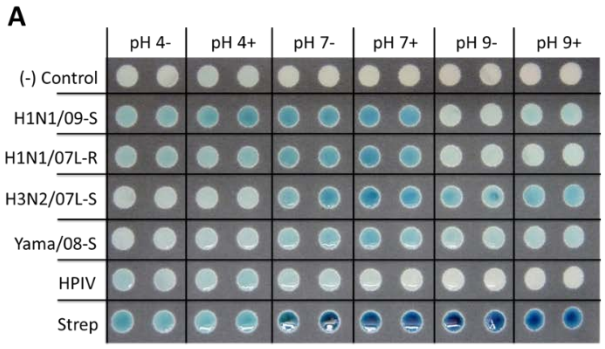

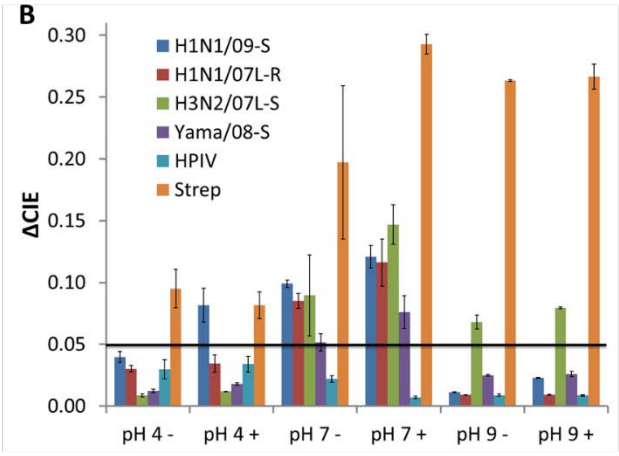

C

Buffer	H1N1/09-S	H1N1/07L-R	H3N2/07L-S	Yama/08-S	HPIV	Strep
pH 4-	-	-	-	-	-	+
pH 4+	+	-	-	-	-	+
pH 7-	+	+	+	-	-	+
pH 7+	+	+	+	+	-	+
pH 9-	-	-	+	-	-	+
pH 9+	-	-	+	-	-	+

Figure 2. Strain Variation in NA Activity due to Different Buffer Conditions. (A) Image of neuraminidase activity assay with buffers at pH of 4, 7, and 9 and either 0.1 mM Ca^{2+} (+) or 5 mM EDTA. (B) Image analysis results (ΔCIE). (C) Summary of a positive or negative NA activity response based on threshold applied to the ΔCIE results (0.05).

Variability of Influenza Type and Subtype Response to Neuraminidase Assay

Initial studies, shown in supplementary information, characterize the neuraminidase activity of influenza NA types. We found that nearly all influenza A and B types have their maximum response in the pH 5-8 range (Figure S5A). Interestingly, the response profile in this pH range for each subtype was uniquely different. In addition, due to NA's dependence on metal cations for proper protein folding and binding to sialic acid, different responses were observed by each type and subtype of influenza when Ca^{+2} or EDTA was present (Figure S5B).

When these two tests were replicated on a paper-based platform, nearly identical results were observed for all influenza types and subtypes, and for the *S. pneumoniae*. These unique responses allow not only for determination as to whether the sample contains influenza or not, but also could potentially allow for initial determination of the type

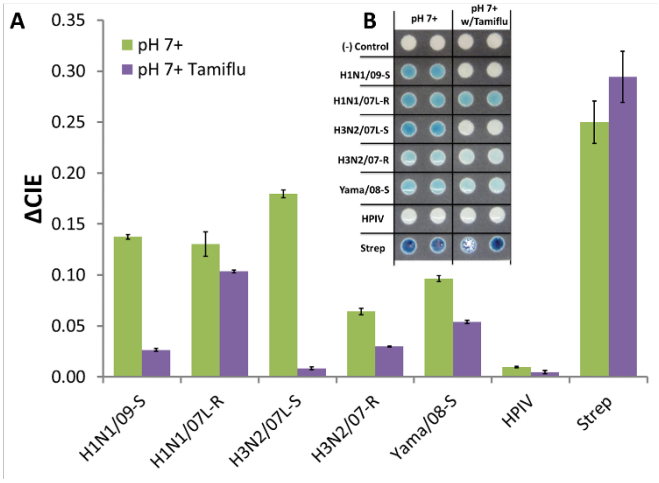

Figure 3. Evaluation of NAI Effectiveness. (A) Image analysis results (ΔCIE) of NA activity at pH 7+ compared to pH 7+ with oseltamivir (Tamiflu) added (350 nM). (B) Corresponding image of NAI effectiveness.

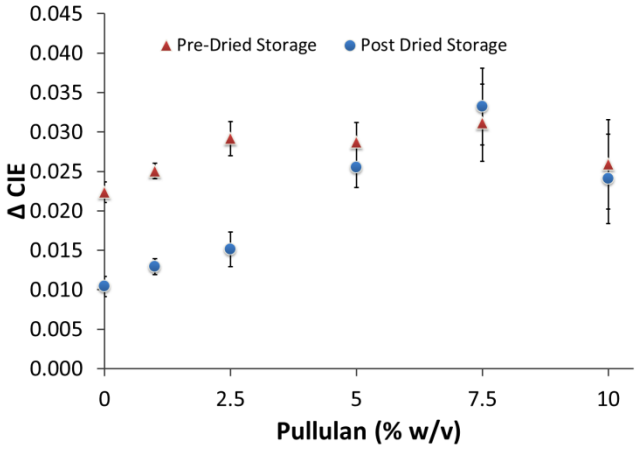

Figure 4. Evaluation of Enzyme Substrate Activity following Storage in Pullulan Matrix. Pullulan was added at increasing concentrations to a non-dried, purified NA / X-NeuNAc reaction to test for potential assay interference (Pre-Dried Storage, red). X-NeuNAc was stored in Pullulan at increasing concentrations to determine proper storage buffer concentration (Post Dried Storage, blue).

neuraminidase present (Type A NA: N1, N2, or Type B NA) (Figure 2A). Surprisingly, the parainfluenza sample did not produce much response on the paper substrate, even at a near optimal pH of 4. The paper substrate is most likely interfering with the binding of the substrate to the HPIV2 NA, which is actually beneficial since HPIV is a potential false positive for influenza neuraminidase activity detection. The other potential false positive, *S. pneumoniae*, does show a strong response across all pH conditions. However, even though it responded at all buffer conditions, this can be used to identify/rule out a sample containing high *S. pneumoniae* concentrations on a POC device since none of the influenza type A and B respond across such a broad range. Through the use of our image analysis methods, thresholds can be set for the amount of color change needed to be considered a positive response (Figure 2B). Finally, using the thresholds set previously, we can see the pattern each influenza type and subtype produce under the different buffer conditions (Figure 2C).

With the design goal of a POC theranostic device, we added physiologically relevant levels of the activated form of Tamiflu®, oseltamivir carboxylate, to the pH 7+ buffer condition which allowed for assessment of influenza NAI susceptibility. Since plasma levels of 180-350 nM have been reported when 75 mg oseltamivir is taken twice daily [15-18], we chose to use 350 nM as our initial test value. For the pH1N1/09-S and H3N2/07L-S, the NA activity was reduced significantly in the presence of the NAI (Figure 3). This was expected since they were previously characterized as being "sensitive" strains to NAIs due to the lack of a reported point mutation of their NA that confer resistance to NAIs. The HPIV did not demonstrate a significant change between non-NAI treated and NAI treated conditions; however, as previously discussed, the HPIV does not produce a strong response on the paper platform, even in optimal pH conditions (Figure 3). Out of the known "resistant" strains, the H1N1/07L-R demonstrated the highest resistance to the NAI (Figure 3). The other two resistant strains, influenza type B Yamagata and H3N2/07-R, both exhibited reduced NA activity in the presence of the NAI even though they contain the reported resistant mutation. Activity in both the Yamagata and H3N2/07-R were reduced to ~50% of their original NA activity with the NAI present (Figure 3). The *S. pneumoniae* was not affected by the NAI, which was expected since the NA on the surface is structurally different from influenza NA and the NAI Tamiflu specifically targets influenza NA. All of these findings very closely match our initial studies on microtiter plates with oseltamivir carboxylate half maximal inhibitory concentration (IC_{50}) results for identical influenza strains (Table S1).

Reagent Preservation and Storage

Multiple enzyme storage mixtures were attempted, with fair to poor results for most of the common reagent preservatives, such as BSA and trehalose. Pullulan, from *Aureobasidium pullulans*, is another sugar-based preservative storage method used previously by another group for enzyme preservation [36]. In their study, they showed very good retention of TaqDP enzyme activity, greater than 90%, even after 50 days of dried storage in Pullulan capsules [36]. We tested the pullulan with the enzyme substrate and purified neuraminidase enzyme in a pre-dried storage assay to verify that there would not be any negative impact to assay performance (Figure 4). Interestingly, at all concentrations of pullulan added to the system, an increase in NA activity was observed. We believe that the long sugar chains of pullulan cause a confinement of the NA and X-NeuNAc into close proximity which enhances reaction rates due to limited diffusion. In addition, considering that the reaction was allowed to proceed until the samples dried, the samples with lower pullulan concentrations dried faster than those with higher concentrations, thus allowing the reaction to proceed

slightly longer due to the prolonged humidity. Both of these thoughts are supported by the fact that there appears to be a concentration dependent response at lower pullulan percentages (0-2.5% w/v), with it leveling off after 2.5% w/v and slightly declining at 10% w/v (Figure 4). The decline at 10% w/v is most likely due to the high viscosity of the solution beginning to have a significant impact on the diffusion of the molecules.

To find the pullulan concentration which was best for storage of the X-NeuNAc, we examined the substrate performance after being dried with increasing concentrations of pullulan onto the paper 96-well plate. After 3 days at room temperature in open air conditions, the samples were resuspended with purified NA was added. The substrate which was stored in the 7.5% w/v pullulan (pH 7+ buffer) gave the highest activity response when the fresh NA was added (Figure 4). While 10% w/v was tested, and it did give second highest activity after dried storage, as mentioned previously, the solution is very viscous and is difficult to pipette accurately. Also, it is very slow to absorb into the filter paper, due to the high viscosity, for loading of the substrate onto the development layer. The 7.5% w/v pullulan concentration was selected as the optimum condition for substrate storage.

Influenza µPAD

The µPAD consists of two wax-patterned filter paper layers and two outside layers of lamination. Following device assembly, 30 µL of DI H_2O containing the virus sample to be tested was added to the µPAD. Initially, very little to no color developed from the substrate in response to the virus sample (Figure S6, Left). Since we had already tested the ability of the dried substrate to resuspend and maintain its activity, we suspected the issue might be within the distribution layer. It was thought that the Whatman filter paper cellulose fibers were non-specifically binding the virus particles and not allowing them to travel to the development layer to react with the substrate. To mitigate this non-specific interaction, we pretreated the distribution layer with 0.5% w/v BSA and 20 mM CTAB to see if either would limit the binding to the cellulose fibers. The BSA treated µPAD produced the best response, with a slight response from the CTAB treated µPAD, which is evident when observing the pH 7+ condition spot (top right spot in the images) (Figure S6, Middle and Right). All distribution layers for any new µPADs were subsequently pretreated with a 0.5% w/v BSA solution.

Once all parameters were optimized for influenza detection, reagent storage, and movement of sample through the µPAD, a final design was determined. The design contains a distribution layer, a development layer, as well as the top and bottom lamination layers. The four test areas in the development layer have an assay control and three different buffer/substrate conditions: pH 7+, pH 7+ with oseltamivir (Tamiflu), and pH 9- (Figures 1C and 5).

The assay control was used to confirm that all reagents in the assay are still viable and that the sample flowed correctly through the µPAD. To accomplish this, purified NA (100 U/mL)

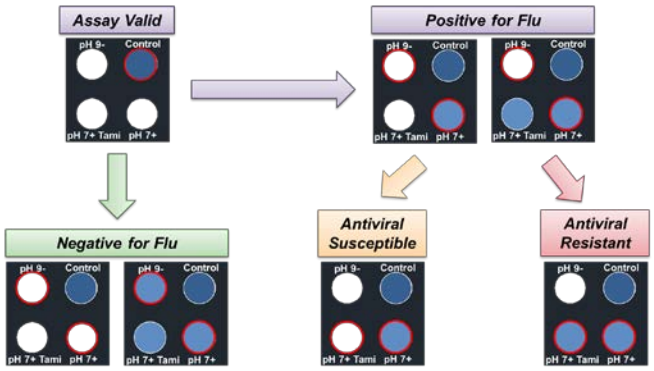

Figure 5. Influenza µPAD Assay Readout. Control spot confirms assay is working properly. Next, top left and bottom right spots are compared to determine if positive (white, blue respectively) or negative (both white or both blue) for influenza. Finally, the bottom left and bottom right spots are compared to determine if the influenza strain is susceptible (white, blue respectively) or resistant (both blue) to the NAI (oseltamivir).

was dried with 7.5% (w/v) pullulan in the distribution layer directly above the control test spot on the development layer, which contained the dried pH 7+ buffer/substrate. When sample is added to the µPAD, the fluid re-suspends the purified NA in the distribution layer and then transfers it to the buffer/substrate in the development layer to produce the control reaction. This is similar to control lines on an LFA style assay to verify that the device and the assay has operated correctly.

The other buffer conditions for the µPAD were taken from the previous optimization work. The pH 7+ buffer/substrate condition was the buffer condition which all of the influenza types tested responded at and was therefore chosen to act as the "positive" condition for influenza. However, since other potential interferents, such as *S. pneumoniae*, are able to respond at the pH 7+ condition, this could create potential false positives for influenza. Thus, we chose the pH 9- buffer/substrate condition to act as a secondary verification for a positive influenza or positive for another NA-containing biological; however, sodium borate buffer was substituted for Tris as the pH 9 buffer due to better stability for storage on the paper. At pH 9-, *S. pneumoniae* responds very strongly while nearly all influenza strains have minimal response. For the pH 7+ with Tamiflu condition, we chose to lower the Tamiflu concentration from 350 nM to 150 nM to give a more accurate representation of NAI effectiveness if used for potential treatment.

To perform a test, 30 µL of DI H_2O containing the diluted virus sample (in a 1:3 ratio) to be tested is added to the µPAD via the sample port on top. The assay was allowed to sit for ~10 h at room temperature prior to imaging. The schematic in Figure 5 describes the visual readout process of the influenza µPAD. First, the control test spot (top right of µPAD) is observed to confirm proper assay function via blue color development. Next, the pH 7+ and the pH 9- test areas (bottom right and top left of µPAD, respectively) are observed

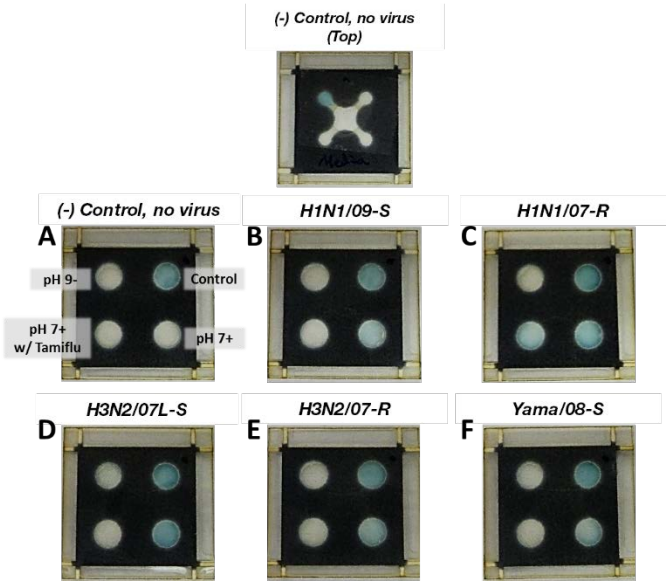

Figure 6. Influenza µPADs Tested with Various Influenza Strains. Top image shows the top view of the negative control µPAD. (A) Negative control. (B) H1N1/09-S. (C) H1N1/07-R. (D) H3N2/07L-S. (E) H3N2/07-R. (F) Yama/08-S.

and compared to determine if the test is positive for influenza (pH 7+: blue, pH 9-: white), positive for another NA-containing biological or a potentially mixed sample (pH 7+: blue, pH 9-: blue; pH 7+: white, pH 9-: blue), or a negative response (pH 7+: white, pH 9-: white).

If the assay shows a positive for influenza, the final step is to determine the NAI susceptibility of the influenza strain being detected for potential therapeutic treatment. By comparing the pH 7+ and pH 7+ with Tamiflu (Tami) test spots, the effectiveness of the NAI on the influenza can be determined. If the pH 7+ spot is blue and the pH 7+ with Tamiflu is blue, then the influenza strain *will not* respond to NAI treatment. Conversely, if the pH 7+ spot is blue and the pH 7+ with Tamiflu spot is white, the influenza strain *is* susceptible to NAIs and they could be used as a therapeutic treatment. Additionally, in the case of a blue response at the pH 7+ condition but a slightly less blue response at the pH 7+ with Tamiflu condition, image analysis can be used to determine an estimate of the NAI treatment effectiveness by comparing the intensity of the blue substrate signal.

When the virus samples were tested, the µPAD responded ideally for all samples tested. All µPADs run indicated valid tests by the blue color development in the control test spot. The negative control media sample (Figure 6A) showed no response in all 3 test areas, indicating the assay functioned properly and that the assay was negative. The H1N1/09-S sample produced a blue response for the pH 7+ condition only, indicating that the sample contains influenza and that the influenza strain detected is susceptible to NAIs (Figure 6B). The H1N1/07L-R µPAD identified that the sample contained influenza (pH 7+: blue) and that the influenza strain detected is mostly NAI resistant. However, using the image analysis data (Figure 6C), we can conclude that 150 nM Tamiflu is able to reduce NA activity by ~40% for the H1N1/07L-R strain. For the H3N2/07L-S, H3N2/07-R, and Yamagata samples, all demonstrated a positive result at the pH 7+ condition only (Figure 6D, 6E, and 6F, respectively), even though H3N2/07-R and Yamagata are both considered resistant strains. As discussed earlier, this is due to the fact that even though their NA has the resistance mutation, their IC_{50}'s are well below 150 nM for oseltamivir (Table S1). Additionally, reduced responses from all strains tested were observed in the µPAD format, which indicates that there may still be some non-specific binding occuring within the device during sample transport, even with the BSA pre-treatment, and may need further studies to minimize. All ΔCIE image analysis results correlate to the visually observed results (Figure S7).

Conclusions

In this work, a novel theranostic µPAD for influenza and NAI susceptibility was demonstrated. We used invariable characteristics of influenza biology (HA and NA) to detect and differentiate influenza virus from HPIV and *S. pneumoniae* by measuring NA activity at different buffer conditions. The use of intrinsic viral characteristics for diagnostic provides a great advantage over antibody-recognition diagnostics, since binding to host factors is not subject to antigenic shift or drift. Moreover, assays performed in the presence and absence of NAI could direct the appropriate use of antiviral therapy.

Optimization of buffer and substrate concentrations for a NA activity assay for integration into a paper-based platform, determined proper incubation temperature for assay performance, and evaluated reagent storage in dried form were performed. Next, while not the primary goal of the work, we demonstrated the ability to differentiate strains of influenza, which could be useful as a clinical laboratory style assay instead of a POC style device. Finally, we designed a µPAD that would allow for simple, one-step addition of sample with the ability to both read the output visually or with the use of image-based analysis to determine if a sample contained influenza, and if it did, also determine the level of NAI susceptibility.

While the reaction time of the assay at this point of development is long compared to current POC influenza assays, the enzymatic influenza detection approach used has numerous advantages over the current antibody-based detection methods. The primary advantage being the ability to not have to redesign the assay every flu season due to the emergence of a new subtype. Additionally, since the assay relies on the NA activity present on the surface of the influenza virus particle, it only detects complete, functioning virus particles and is able to directly indicate the effectiveness of antiviral therapeutics (NAIs).

For human mucosal sample testing, a buffer solution would be necessary to dilute the nasal swab into prior to introduction into the device. This buffer solution would not only reduce the high viscosity of the mucosal sample, but it would also stabilize the pH and could as potentially be used to help minimize/remove potential assay interferents.

Future work in this area will primarily focus on reduction of assay time through investigation of alternate substrates, possibly fluorescent or chemiluminescent, or the incorporation of electrochemical detection capabilities into the µPAD to increase detection sensitivity. Most likely a voltammetry-type measurement will be used to determine amounts of NA activity. Additionally, real patient mucosal samples will be evaluated in future studies, possibly as part of a clinical trial.

Acknowledgements

The authors would like to acknowledge that this work was supported by AFRL and NIH grant R01AI089450. Also, the authors would like to acknowledge the device fabrication support and facilities from the University of Cincinnati Ohio Center for Microfluidic Innovation (OCMI).

Notes and references

1. M. N. Matrosovich, T. Y. Matrosovich, T. Gray, N. A. Roberts and H.-D. Klenk, *Proceedings of the National Academy of Sciences of the United States of America*, 2004, **101**, 4620-4624.
2. N.-A. M. Molinari, I. R. Ortega-Sanchez, M. L. Messonnier, W. W. Thompson, P. M. Wortley, E. Weintraub and C. B. Bridges, *Vaccine*, 2007, **25**, 5086-5096.
3. P. D. Stahl and R. A. B. Ezekowitz, *Current Opinion in Immunology*, 1998, **10**, 50-55.
4. M. Ohuchi, N. Asaoka, T. Sakai and R. Ohuchi, *Microbes and Infection*, 2006, **8**, 1287-1293.
5. M. N. Matrosovich, *J Virol*, 2004, **78**, 12665-12667.
6. E. De Clercq, *Nat Rev Drug Discov*, 2006, **5**, 1015-1025.
7. G. L. Mandell, R. G. Douglas and J. E. Bennett, *Mandell, Douglas, and Bennett's Principles and Practice of Infectious Diseases*, Churchill Livingstone, An Imprint of Elsevier Philadelphia, PA, 7th edition edn., 2010.
8. I. V. Alymova, G. Taylor and A. Portner, *Current Drug Targets - Infectious Disorders*, 2005, **5**, 401-409.
9. S. Richards, *Journal*, 2012, **61**, 619-621.
10. D. Jan Felix, H. Angelika, K. Heike, R. Ulrike, P. Marcus, A. M. Marcel, H. Katja, M. Bertfried, P. Sung Sup and E.-H. Anna Maria, *Emerging Infectious Disease journal*, 2009, **15**, 1662.
11. K. Tsui-Mai, W. Un-In and C. Yee-Chun, *Emerging Infectious Disease journal*, 2010, **16**, 1181.
12. Y. Sakai-Tagawa, M. Ozawa, D. Tamura, M. t. Q. Le, C. A. Nidom, N. Sugaya and Y. Kawaoka, *Journal of Clinical Microbiology*, 2010, **48**, 2872-2877.
13. A. Balish, R. Garten, A. Klimov and J. Villanueva, *Influenza and Other Respiratory Viruses*, 2012, DOI: 10.1111/irv.12017, no-no.
14. A. W. Martinez, S. T. Phillips, M. J. Butte and G. M. Whitesides, *Angewandte Chemie*, 2007, **119**, 1340-1342.
15. D. A. Bruzewicz, M. Reches and G. M. Whitesides, *Analytical Chemistry*, 2008, **80**, 3387-3392.
16. S. Wang, F. Xu and U. Demirci, *Biotechnology Advances*, 2010, **28**, 770-781.
17. M. A. Alyassin, S. Moon, H. O. Keles, F. Manzur, R. L. Lin, E. Haeggstrom, D. R. Kuritzkes and U. Demirci, *Lab on a Chip*, 2009, **9**, 3364-3369.
18. C.-M. Cheng, A. W. Martinez, J. Gong, C. R. Mace, S. T. Phillips, E. Carrilho, K. A. Mirica and G. M. Whitesides, *Angewandte Chemie International Edition*, 2010, **49**, 4771-4774.
19. A. W. Martinez, *Bioanalysis*, 2011, **3**, 2589-2592.
20. R. C. Murdock, L. Shen, D. K. Griffin, N. Kelley-Loughnane, I. Papautsky and J. A. Hagen, *Analytical Chemistry*, 2013, **85**, 11634-11642.
21. S. Wang, L. Ge, X. Song, J. Yu, S. Ge, J. Huang and F. Zeng, *Biosensors and bioelectronics*, 2012, **31**, 212-218.
22. W. Wang, W.-Y. Wu, W. Wang and J.-J. Zhu, *Journal of Chromatography A*, 2010, **1217**, 3896-3899.
23. D.-S. Lee, B. G. Jeon, C. Ihm, J.-K. Park and M. Y. Jung, *Lab on a Chip*, 2011, **11**, 120-126.
24. M. A. Nash, J. M. Hoffman, D. Y. Stevens, A. S. Hoffman, P. S. Stayton and P. Yager, *Lab on a Chip*, 2010, **10**, 2279-2282.
25. W. G. Lee, Y.-G. Kim, B. G. Chung, U. Demirci and A. Khademhosseini, *Advanced Drug Delivery Reviews*, 2010, **62**, 449-457.
26. A. W. Martinez, S. T. Phillips, G. M. Whitesides and E. Carrilho, *Analytical Chemistry*, 2010, **82**, 3-10.
27. E. K. Sackmann, A. L. Fulton and D. J. Beebe, *Nature*, 2014, **507**, 181-189.
28. A. W. Martinez, S. T. Phillips, E. Carrilho, S. W. Thomas, H. Sindi and G. M. Whitesides, *Analytical Chemistry*, 2008, **80**, 3699-3707.
29. D. M. Cate, J. A. Adkins, J. Mettakoonpitak and C. S. Henry, *Analytical chemistry*, 2014, **87**, 19-41.
30. A. K. Yetisen, M. S. Akram and C. R. Lowe, *Lab on a Chip*, 2013, **13**, 2210-2251.
31. E. Vimr, *Trends in microbiology (Regular ed.)*, 2002, **10**, 254-257.
32. V. P. Mishin, M. Watanabe, G. Taylor, J. DeVincenzo, M. Bose, A. Portner and I. V. Alymova, *Journal of virology*, 2010, **84**, 3094-3100.
33. G. Xu, M. J. Kiefel, J. C. Wilson, P. W. Andrew, M. R. Oggioni and G. L. Taylor, *Journal of the American Chemical Society*, 2011, **133**, 1718-1721.
34. A. M. Berry, R. A. Lock and J. C. Paton, *Journal of Bacteriology*, 1996, **178**, 4854-4860.
35. D. Parker, *Infection and immunity*, 2009, **77**, 3722-3730.
36. S. Jahanshahi-Anbuhi, K. Pennings, V. Leung, M. Liu, C. Carrasquilla, B. Kannan, Y. Li, R. Pelton, J. D. Brennan and C. D. M. Filipe, *Angewandte Chemie*, 2014, **126**, 6269-6272.

